Science and Technology Infusion Climate Bulletin
NOAA's National Weather Service
40th NOAA Annual Climate Diagnostics and Prediction Workshop
Denver, CO, 26-29 October 2015

Teleconnection Patterns Impacting on the Summer Consecutive Extreme Rainfall in Central-Eastern China

Junmei Lü[1,2], Yun Li[2], Panmao Zhai[1*], Junming Chen[1], and Tongtiegang Zhao[2]
[1]*Chinese Academy of Meteorological Sciences, Beijing, China*
[2]*CSIRO Mathematics, Informatics and Statistics, Wembley, Western Australia, Australia*

1. Introduction

Extreme weather and climate events such as deadly heat waves, devastating floods and severe droughts can damage human societies and ecosystems. Numerous previous studies have demonstrated that there has been an increase in the frequency and intensity of extreme weather events in recent decades (Meehl *et al.* 2000; Zhai *et al.* 2005; Fischer *et al.* 2007; Kyselý 2008). For instance, heat waves have become longer and hotter, and heavy rains and flooding have become more intense and more frequent. Consecutive extreme rainfall (CER) events, which usually cause large-scale floods, mudflows and landslides, are defined as "consecutive rainfall persisting for at least 3 days with the daily rainfall exceeding 50 mm" (Chen and Zhai 2013). Chen and Zhai (2013) proposed that individual-station-based CER events occurred mainly in Central-Eastern and South China, which are the most populated and economically developed regions in China.

Recent studies have shown that the large-scale systems that produce CER are often related to anomalous and persistent atmospheric wave patterns such as blocking anticyclones and cutoff lows, which are characterized by slow moving or stagnant features and related to teleconnection patterns (Zhou *et al.* 2009; Lau and Kim 2012； Chen and Zhai 2014). The goal of this study is to investigate the dominant modes of the CER over Central-Eastern China and to identify their corresponding persistent circulation patterns. The impacts of anomalous SSTs and Rossby wave propagation on the formation of teleconnection patterns are also discussed.

2. Methodology

The 95th percentile is widely used to evaluate the threshold for extreme rainfall. Chen and Zhai (2013) calculated the 95th percentile of daily total precipitation in China during the warm season and found that a daily precipitation amount of 50 mm exceeded the 95th percentile at over 90% of stations. Hence, the absolute threshold of extreme rainfall is defined as exceeding 50 mm for daily total precipitation. The CER events over Central-Eastern China are defined according to the following criteria: (1) the JJA daily rainfall exceeds 50 mm at one or more weather stations, (2) the extreme rainfall persists for at least 3 consecutive days, and (3) the CER events end when daily rainfall is less than 50 mm d^{-1} over 2 consecutive days. This definition ensures the regional occurrences of CER events.

The CER event definition was applied to a 32-year period (1979-2010) for 210 weather stations. This analysis resulted in 86 CER events and 340 event days. Empirical orthogonal function (EOF) analysis was performed on 230 event days to assess the dominant modes of the CER (EOFs) and their corresponding time series (PCs). The relationship between various circulation patterns and the CER modes was determined by correlating grid-point anomalies of an atmospheric field onto an index, for example, the PC of an EOF, or the SST index. To find out the mechanisms that maintain the teleconnection wave trains associated with CER events, we analyzed the wave-activity flux formulated by Takaya and Nakamura (2001) and the ray paths derived by Hoskins and Karoly (1981). Ray equations for stationary waves were given by Wang *et al.* (2007).

3. Analysis

An EOF analysis of the CER revealed three dominant modes that together account for 44% of the total CER variance (Fig. 1 left panels). The first mode represents the consistent changes in the CER events over the

[*]Correspondence to: Panmao Zhai, State Key Laboratory of Severe Weather, Chinese Academy of Meteorological Sciences, 46 Zhong-guan-cun-nan-da-jie, Haidian, Beijing 100081, China; E-mail: pmzhai@cma.gov.cn.

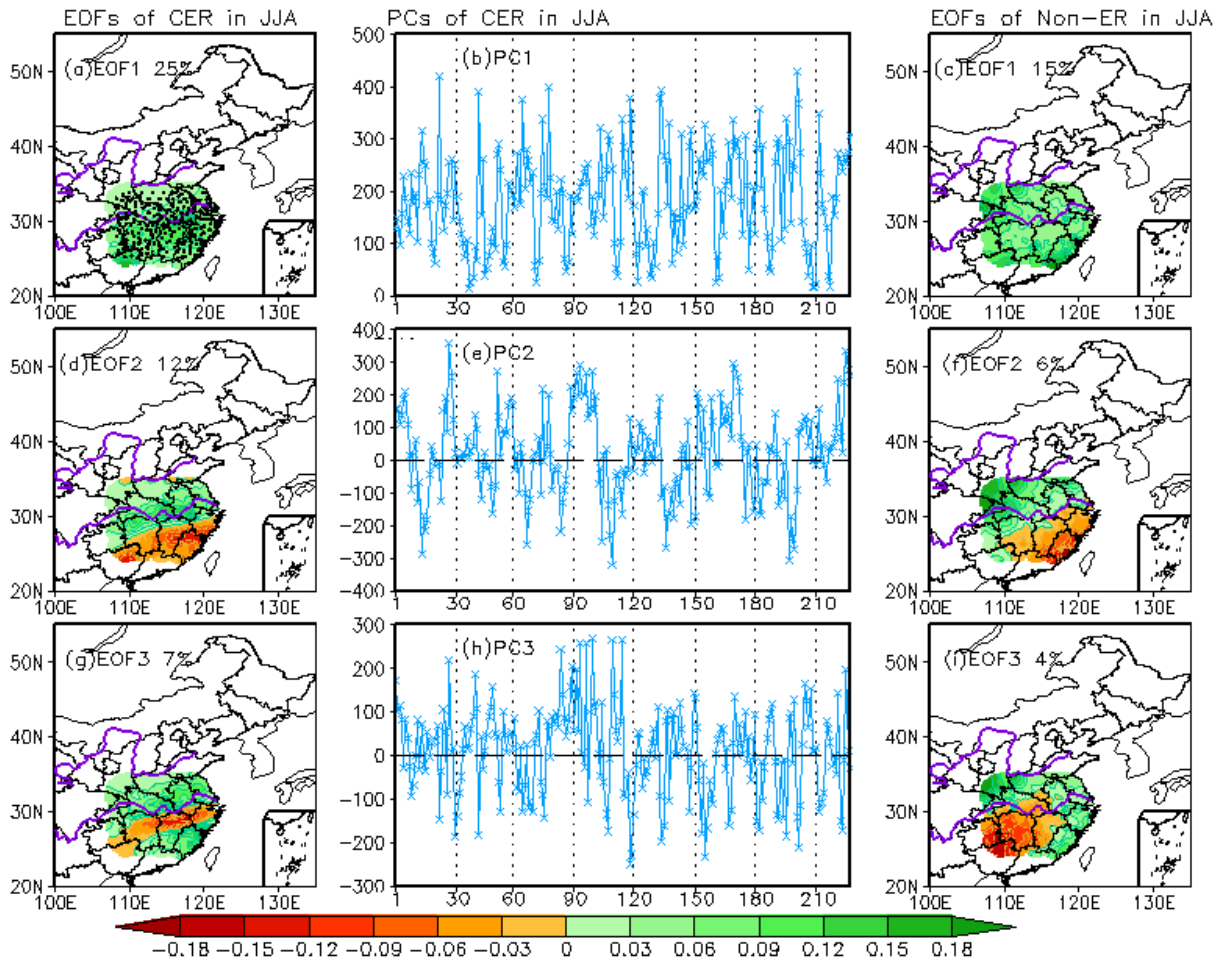

Fig. 1 The EOF modes of the CER (left panels), PCs of the CER (middle panels), and EOF modes of non-ER rainfall (right panels) during JJA. The explained variance of each EOF is indicated at the top. Closed circles in (a) show the locations of the 210 observation stations in Central-Eastern China.

entire region (Fig. 1a). This mode suggests a climate status that is related to the occurrence of CER events over the entire area. The second mode has a dipolar structure with inverse variations of the CER in the southern Yangtze River (SYR) and the Yangtze-Huaihe River Valley (YHRV) (Fig. 1d). The third mode is characterized by a tripolar structure (Fig. 1g). To compare the dominant modes of the CER versus non-extreme rainfall (non-ER, <50 mm d^{-1}), the three leading EOFs of non-ER are also shown in Fig. 1 (right panels). The three leading EOFs of non-ER explain just 25% of the total non-ER variance, which is much less than 44% for the CER. Although the first mode of non-ER (Fig. 1c) has a uniform regional variation similar to the first mode for the CER, the spatial correlation between the two EOF1 patterns is -0.16, suggesting that the two types of rainfall have totally different distributions. For example, the highest rainfall value is located in the center of the area for the CER (Fig. 1a), while the highest values for the non-ER are located in the northwestern and southeastern corners (Fig. 1c). The second mode of non-ER has a dipolar structure (Fig. 1f) and significantly correlates with the second mode of the CER (r=0.55). The third mode of non-ER (Fig. 1i) does not share the tripolar structure of the EOF3 for the CER, although there is a significant correlation between the two EOFs (r=0.31). These differences demonstrate the importance of rainfall type classification according to rainfall intensity.

To derive teleconnection pattern associated with the first mode of the CER, one-point correlation is performed on 500 hPa geopotential height anomalies at days -6, -4, -2 and 0 with reference to the base point denoted by the box [28°- 43° N, 130°- 160° W] in Fig. 2 a-b, and another box [20°- 35° N, 130°- 160° W] in

Fig. 2 c-d. A barotropic circumglobal teleconnection (CGT) pattern with a zonal wavenumber-3 structure occurs from days -6 to 0. Pressure variations over northeastern North America, the North Atlantic, and the Caspian Sea are all in phase with variation over the subtropical North Pacific (SNP), as shown by significant positive correlations. In contrast, pressure fluctuations over North America, northwestern Europe, and the Lake Baikal-East Asia area exhibit significant negative correlations. Ding and Wang (2005) also found that a CGT pattern with a zonal wavenumber-5 structure exists during boreal summer. This CGT influences rainfall and temperature in continental regions including East Asia.

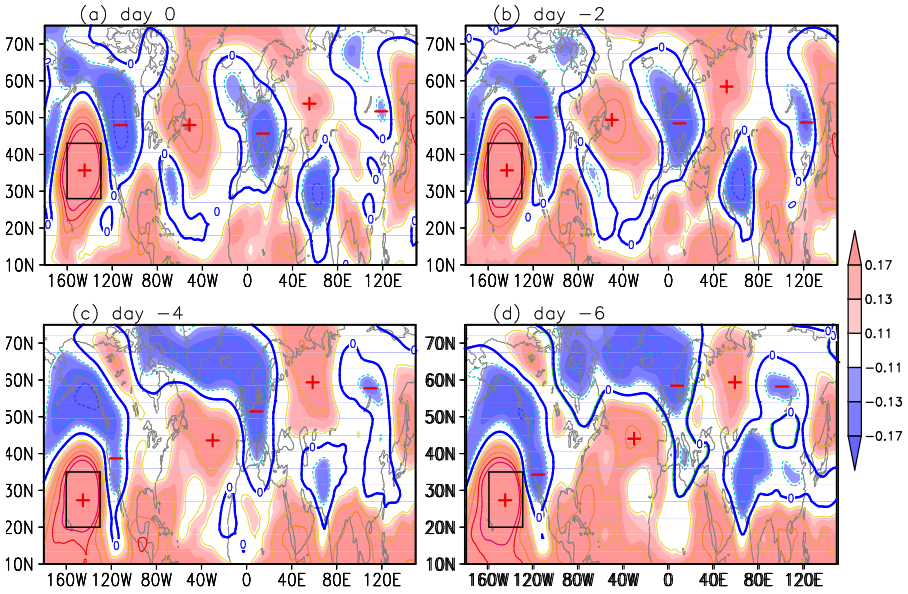

Fig. 2 One-point correlation map between the base point (box) and 500 hPa geopotential height anomalies at day 0 (a), day -2 (b), day -4 (c), and day -6 (d). Shaded areas denote significance at the 0.10, 0.05 and 0.01 levels.

The second mode of the CER shows inverse variations in the SYR and the YHRV. Fig. 3 displays the one-point correlation between the base point (15°- 25° N, 90°- 130° E) and 500 hPa geopotential height anomalies at lags of 0, -5, -10, and -15 days. It is apparent that a negative Pacific-Japan (PJ) teleconnection pattern occurs 15 days prior to the CER events and maintains this wave train thereafter.

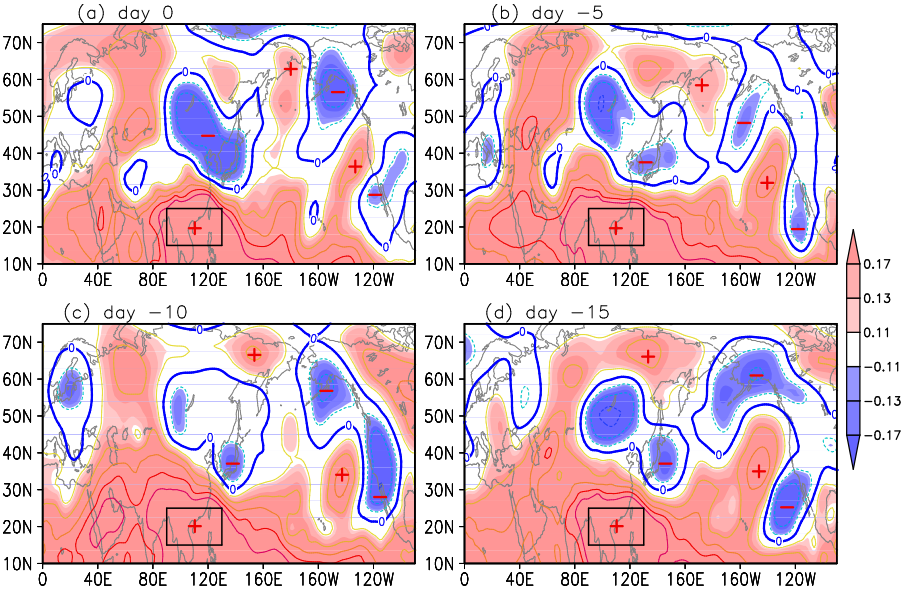

Fig. 3 One-point correlation map between the base point (box) and 500 hPa geopotential height anomalies for day 0 (a), day -5 (b), day -10 (c), and day -15 (d). Shaded areas indicate significance at the 0.10, 0.05 and 0.01 levels.

The third mode of the CER events indicates that the probability of CER occurring in the YRV is low, while it is high in the Huaihe River Valley (HRV) and the SYR. As shown in Fig. 4, a negative Eurasian pattern (EU) exists at lags of -6, -4, -2 and 0 days. Significant negative correlations are located in the northeastern Atlantic and the area east of the Caspian Sea to Lake Baikal. On the other hand, significant positive correlations exist over the Mediterranean Sea to Western Europe and East Asia. It should be noted that the positive correlation over the East Asia is related to the Bonin high, suggesting that the negative EU-like teleconnection plays an important role on the formation of the Bonin high.

4. Concluding remarks

In this study, CER events over Central-Eastern China during the period from 1979-2010 were identified based on the new definition. The dominant modes of the CER were determined based on EOF analysis. Our results show that the spatial distribution of the CER can be attributed to certain persistent circulation patterns, which makes sense because prolonged weather conditions can enhance the possibility of extreme events. When CER events occur over the entire region, the Western Pacific Subtropical High (WPSH) prevails in South China and the northern South China Sea (SCS); 5 days prior to CER event onset, the WPSH is located in the middle of the SCS, after which it migrates northward, bringing water vapor from the western North Pacific (WNP) to the SYR and then the YHRV. Additionally, a barotropic CGT pattern with two major components, namely the Lake Baikal trough and the Ural blocking high, is found in geopotential height and persists from days -6 to 0. On the other hand, a negative PJ pattern is identified in geopotential height 15 days before the CER events occur over the YHRV. The WPSH, blocking high around the Sea of Okhotsk, and the anomalous low pressure south of Lake Baikal are three components of the negative PJ pattern. Furthermore, double blocking highs appear around the Ural mountains and the Sea of Okhotsk, distinguishing the persistent circulations of the second CER mode from the first mode. Moisture convergence and ascending motion anomalies prevail over the YHRV 5 days prior to CER event onset, accompanying the northwestward extension of the WPSH from the WNP to South China and the SYR. The third mode is associated with a negative EU-like teleconnection that appears 6 days before CER event onset. As one component of the EU-like teleconnection, the Bonin high covers East Asia from days -5 to 0 with moisture convergence and ascending motion anomalies over the HRV and SYR. This configuration of circulation anomalies favors the occurrence of CER events over the HRV and SYR. Thus, the configuration of persistent circulation anomalies is responsible for the CER distributions.

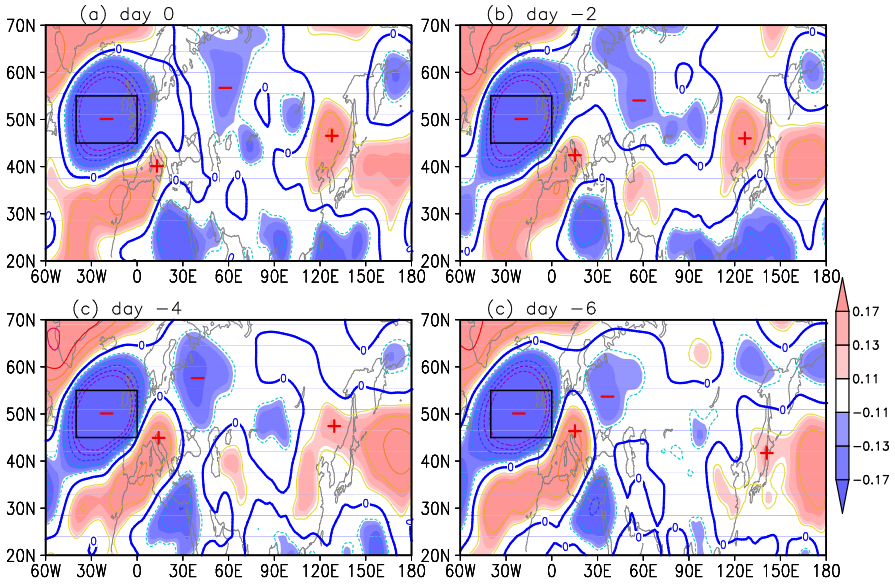

Fig. 4 One-point correlation map between the base point (box) and 500 hPa geopotential height anomalies for day 0 (a), day -2 (b), day -4 (c), and day -6 (d). Shaded areas indicate significance at the 0.10, 0.05 and 0.01 levels.

Rossby wave propagation plays a key role in the formation and persistence of teleconnection patterns. Note that the three teleconnection patterns associated with the three CER modes are induced by SST anomalies around their base points. The ray paths based on these three base points correspond to the CGT, PJ and EU wave trains, suggesting the importance of propagating Rossby waves for the formation of teleconnection patterns, although the mechanism through which stationary Rossby waves respond to these heat sources needs to be investigated further.

References

Chen Y., and P. M. Zhai, 2013: Persistent extreme precipitation events in China during 1951-2010. *Clim. Res.*, **57**, 143–155, doi: 10.3354/cr01171.

Chen Y., and P. M. Zhai, 2014: Precursor circulation features for persistent extreme precipitation in Central-Eastern China. *Wea. Forecasting*, **29**, 226–240, doi: 10.1175/ WAF-D-13-00065.1.

Ding, Q. H., and B. Wang, 2005: Circumglobal teleconnection in the Northern Hemisphere summer. *J. Climate*, **18**, 3483–3505, doi: 10.1175/JCLI3473.1.

Fischer, E. M., Seneviratne S. I., Lüthi D., and Schär C., 2007: Contribution of land- atmosphere coupling to recent European summer heat waves. *Geophys. Res. Lett.,* **34**, L06707, doi: 10.1029/2006GL029068.

Hoskins, B. J., and Karoly, D. J., 1981: The steady linear response of a spherical atmosphere to thermal and orographic forcing. *J. Atmos. Sci.*, **38**: 1179–1196,
doi: 10. 1175/1520-0469(1980)038<1179.TSLROA>2.0.CO:2

Kyselý, J. 2008: Influence of the persistence of circulation patterns on warm and cold temperature anomalies in Europe: Analysis over the 20th century. *Global and Planetary Change*, **62**, 147–163, doi: 10.1016/j.gloplacha.2008.01.003.

Lau, W. K. M., and K.-M. Kim, 2012: The 2010 Pakistan flood and Russian heat wave: teleconnection of hydrometeorological extremes. *J. Hydrometeor.*, **13**: 392– 403, doi: 10.1175/JHM-D-11-016.1.

Meehl, Gerald A., and Coauthors, 2000: An introduction to trends in extreme weather and climate events: observations, socioeconomic impacts, terrestrial ecological impacts, and model projections. *Bull. Amer. Meteor. Soc.*, **81**, 413–416, doi: 10.1175/1520- 0477(2000)081<413.TSLROA>2.0.CO:2.

Takaya, K., and H. Nakamura, 2001: A formulation of a phase-independent wave-activity flux for stationary and migratory quasigeostrophic eddies on a zonally varying basic flow. *J. Atmos. Sci.*, **58**, 608–627, doi: 10.1175/1520-0469 (2001)058<0608: AFOAPI>2.0.CO;2.

Wang Y., K. Yamazaki, and Y. Fujiyoshi, 2007: The interaction between two separate propagations of Rossby waves. *Mon. Wea. Rev.*, **135**, 3521–3540, doi: 10.1175/MWR3486.1.

Zhai, P. M., X. B. Zhang, H. Wan, and X. H. Pan, 2005: Trends in total precipitation and frequency of daily precipitation extremes over China. *J. Climate*, **18**, 1096–1108, doi: 10.1175/JCLI-3318.1.

Zhou, W., J.C. L. Chan, W. Chen, J. Ling, J. G. Pinto, and Y. P. Shao. 2009: Synoptic-scale controls of persistent low temperature and icy weather over southern China in January 2008. *Mon. Wea. Rev.*, **137**: 3978–3991, doi: 10.1175/2009MWR 2952.1.